Neptunium and manganese biocycling in nuclear legacy sediment systems

Clare L. Thorpe [a], Katherine Morris [a], Jonathan R. Lloyd [a], Melissa A. Denecke [b], Kathleen A. Law [b], Kathy Dardenne [c], Christopher Boothman [a], Pieter Bots [a], Gareth T.W. Law [b, *]

[a] Research Centre for Radwaste Disposal and Williamson Research Centre for Molecular Environmental Science, School of Earth, Atmospheric and Environmental Sciences, The University of Manchester, Manchester M13 9PL, UK
[b] Centre for Radiochemistry Research, School of Chemistry, The University of Manchester, M13 9PL, UK
[c] Karlsruhe Institute of Technology, Institut Fur Nukleare Entsorgung, D-76021 Karlsruhe, Germany

ARTICLE INFO

Keywords:
Neptunium
Contaminated land
Biostimulation

ABSTRACT

Understanding the behaviour of the highly radiotoxic, long half life radionuclide neptunium in the environment is important for the management of radioactively contaminated land and the safe disposal of radioactive wastes. Recent studies have identified that microbial reduction can reduce the mobility of neptunium *via* reduction of soluble Np(V) to poorly soluble Np(IV), with coupling to both Mn and Fe(III) reduction implicated in neptunyl reduction. To further explore these processes Mn(IV) as δMnO_2 was added to sediment microcosms to create a sediment microcosm experiment "poised" under Mn reducing conditions. Enhanced removal of Np(V) from solution occurred during Mn reduction, and parallel X ray absorption spectroscopy (XAS) studies confirmed Np(V) reduction to Np(IV) commensurate with microbially mediated Mn reduction. Molecular ecology analysis of the XAS systems, which contained up to 0.2 mM Np showed no significant impact of elevated Np concentrations on the microbial population. These results demonstrate the importance of Mn cycling on Np biogeochemistry, and clearly highlight new pathways to reductive immobilisation for this highly radiotoxic actinide.

1. Introduction

Internationally, deep geological disposal is being considered as the long term management and disposal option for higher activity radioactive wastes (HAW). A fundamental knowledge of reactions between radionuclides and geomedia is essential to underpin the safety case for geodisposal. Neptunium is a key risk driving radio nuclide in HAW due to its long half life (^{237}Np t½ 2.1 × 10^6 years), ingrowth from ^{241}Am, high radiotoxicity, and relatively high solu bility as Np(V). Indeed, Np is potentially the most mobile trans uranic species in environments pertinant to deep geological disposal (e.g. Choppin and Stout, 1989; Kaszuba and Runde, 1999; Lloyd et al., 2000; Choppin, 2007; Law et al., 2010); further, Np is a persistant contaminant at or near nuclear sites (e.g. Cantrell, 2009; Morris et al., 2000; Stamper et al., 2013).

Neptunium is redox active and it's environmental mobility can be affected by the biogeochmistry and redox conditions in the subsurface (Kaszuba and Runde, 1999; Lloyd et al., 2002; Choppin, 2007; Law et al., 2010). Under oxidising conditions Np is stable in solution as the soluble neptunyl cation, NpO_2^+, whilst under anaerobic conditions Np can be reduced to poorly soluble Np(IV) species (Kaszuba and Runde, 1999; Moyes et al., 2002; Llorens et al., 2005; Law et al., 2010; Bach et al., 2014). In the subsurface, mi crobial respiration can induce anaerobic conditions under which metals and radionuclides can be reduced (Lloyd and Renshaw, 2005). The development of bioreducing conditions is increasingly recognised as likely to be significant in the deep subsurface around a geological disposal facility (Pedersen, 2000; Fredrickson and Balkwill, 2006; Rizoulis et al., 2012; Williamson et al., 2013; Behrends et al., 2012), and is the basis for remediation of contam inated land where problematic radionuclides (e.g. Tc and U) may be reduced either enzymatically or indirectly *via* interactions with reduced species (e.g. Fe(II): Lloyd et al., 2002; Lloyd, 2003; Gadd, 2010; Newsome et al., 2014).

* Corresponding author.
E-mail address: gareth.law@manchester.ac.uk (G.T.W. Law).

The ability of microorganisms to enzymatically reduce Np(V) to Np(IV) has been demonstrated in pure culture experiments (Lloyd et al., 2000; Icopini et al., 2007) although some microorganisms are unable to facilitate enzymatic Np(V) reduction (Songkasiri et al., 2002; Renshaw et al., 2005). In contrast, Gorman Lewis et al. (2005) inferred potential non enzymatic reduction of Np(V) to explain trends in sorption/desorption experiments conducted with *Bacillus subtilis*. Toxicity effects on selected metal reducing bacteria are also of interest as studies with indigenous microorganisms highlight the tolerence of microorganisms to mM concentrations of Np (Law et al., 2010; Ams et al., 2013), whilst in pure culture experiments no toxicity effects were observed at Np concentrations less than 2 mM (Ruggiero et al., 2005). In sediment systems, reductive immobilisation of Np(V) to Np(IV) has been observed during development of sediment anoxia with microbial metal reduction implicated in the reaction and with indirect (abiotic) reduction by Fe(II) shown to be possible (Law et al., 2010).

Manganese is ubiquitous in soils and rock forming minerals and therefore, although Np interactions with Mn minerals have been studied previously (Wilk et al., 2005), a deeper understanding of Np(V) behaviour during early metal reduction (Mn and Fe(III) reduction) is essential in understanding its environmental behaviour in both deep and shallow subsurface environments. In addition, the potential importance of Mn in environmental actinide chemistry is increasingly recognised with Mn linked to both Pu and U cycling (Powell et al., 2006; Hu et al., 2010; Wang et al., 2013, 2014). Here we examine the behaviour of Np in sediment systems amended with labile Mn(IV) (δMnO_2) to allow microcosms to develop a period of extended or "poised" Mn reduction (Lovley and Phillips, 1988). As well conducting experiments at low Np concentrations, we also collected XAS data from parallel experiments run at higher concentrations of Np. This allowed assessment of Np speciation and local coordination under defined biogeochemical conditions. Finally, 16S rRNA gene analysis was performed to assess the response of the indigenous microbial communities to elevated Np concentrations.

2. Experimental section

2.1. Safety

Neptunium (^{237}Np) is a high radiotoxicity alpha emitting radionuclide with beta/gamma emitting progeny. Work can only be conducted by trained personnel in a certified, properly equipped radiochemistry laboratory, following appropriate risk assessment. The possession and use of radioactive materials is subject to statutory control.

2.2. Sample collection

Sediments were collected from an area located ~2 km from the Sellafield reprocessing site in Calder River Valley, Cumbria (Lat 54°26′30 N, Long 03°28′09 W). Sediments were representative of the Quaternary unconsolidated alluvial flood plain deposits that underlie the Sellafield site (Law et al., 2010) and were collected in sterile containers, sealed, and stored at 4 °C prior to use (<1 month).

2.3. Bioreduction microcosms with low NpO_2^+ concentrations

Sediment microcosms (10 ± 0.1 g Sellafield sediment, 100 ± 1 ml groundwater; in triplicate) were prepared using a synthetic groundwater representative of the Sellafield region (Wilkins et al., 2007) but with added nitrate and manganese (2 mM $NaNO_3$, 2 mM δMnO_2) and with a total 0.17 mmols of bioavailable Fe(III) in the sediment. Sodium acetate was also added in stoichiometric excess (10 mM) as an electron donor, the groundwater was sterilised (autoclaved for 1 h at 120 °C), purged with filtered 80%/20% N_2/CO_2, and pH adjusted to pH 7 (*via* drop wise addition of 0.5 M HCl or 1 M NaOH). Sediments and sterile groundwater were then added to sterile 120 ml glass serum bottles (Wheaton Scientific, USA) and sealed with butyl rubber stoppers using aseptic technique. Neptunium, as $^{237}NpO_2^+$ (20 Bq ml^{-1}; 3.2 μM; oxidation state verified by UV–Vis analysis) was then spiked into each microcosm; thereafter, the microcosms were incubated anaerobically at 21 °C in the dark for 38 days. Throughout the incubation, sediment slurry was periodically extracted using aseptic technique, under an O_2 free, Ar atmosphere. The sediment slurry was centrifuged (15,000 g; 10 min) to separate sediment and porewater samples and ~0.5 g of sediment was stored at 80 °C for later microbiological characterisation.

2.4. Geochemical analyses

During microcosm sampling, total dissolved Mn and Fe concentrations were measured with standard UV–Vis spectroscopy methods on a Jenway 6715 spectrophotometer (Lovley and Phillips, 1987; Goto et al., 1997; Viollier et al., 2000). Aqueous NO_3^-, SO_4^{2-}, ammonium and acetate were measured by ion chromatography (Dionex ICS5000). Total bioavailable Fe(III) and the proportion of extractable Fe(II) in the sediment was estimated by digestion of 0.1 g of sediment in 5 ml of 0.5 N HCl for 60 min followed by the ferrozine assay, with and without added hydroxylammonium chloride (Lovley and Phillips, 1987; Viollier et al., 2000). The pH and Eh were measured with an Orion 420A digital meter and calibrated electrodes. Standards were routinely used to check the reliability of all methods and typically, calibration regressions had $R^2 \geq 0.99$. The elemental composition and bulk mineralogy of the sediment were determined by XRF (Thermo ARL 9400) and XRD (Philips PW 1050). Total organic carbon and total inorganic carbon were determined on a LECO CR 412 Carbon Analyser. The total ^{237}Np concentration in solution was measured by ICP MS (Agilent 7500cx) using ^{232}Th as the internal standard.

2.5. XAS experiments

Experiments were prepared to allow direct determination of Np speciation and local coordination environment in sediments under different geochemical conditions using X ray Absorption Spectroscopy (XAS). Here, the elevated concentration of Np required for direct spectroscopic characterisation (0.2 mM Np(V) as NpO_2^+ in 0.07 M HCl) was added to microcosms containing 1 g of sediment and 10 ml of groundwater that were poised at oxic, nitrate , Mn , Fe(III) , and sulphate reducing conditions, respectively. After Np(V) addition, the microcosms were left to incubate for 1 week in the dark at 7 °C prior to geochemical sampling and subsequent freezing at 80 °C. Two additional Mn reducing XAS systems were also established where sediments had 2 mM of δMnO_2 added: (i) 0.2 mM NpO_2^+ was added to an oxic microcosm that was then left to progress to Mn reducing conditions (verified by the presence of Mn in porewaters and the absence of detectable 0.5 N extractable Fe(II) in sediments) before freezing at 80 °C, and (ii) a parallel Mn reducing microcosm (again with no detectable 0.5 N extractable Fe(II) in sediments) that was sterilised by autoclaving (1 h at 120 °C) prior to the addition of 0.2 mM NpO_2^+, and which was frozen at 80 °C 2 days after Np(V) addition. For XAS analysis, sediment samples were defrosted, centrifuged, and ~0.5 g of sediment was packed (under anaerobic atmosphere if necessary) into airtight sample containers which were then triple contained and frozen until analysis. XAS analysis was conducted at the INE Beamline for

Actinide Research at the ANKA synchrotron, Karlsruhe, Germany. Neptunium L_{III} edge spectra (17,610 eV) were collected in fluorescence mode by a 5 element solid state Ge detector. Parallel K edge measurements from a Zr foil were recorded for energy calibration. XANES data were collected for all samples and EXAFS data were collected for selected samples. Background subtraction, data normalization, and fitting to EXAFS spectra were performed using the software packages Athena and Artemis. The XANES edge jump was tied to unity. Modelling of the EXAFS data in k^3 range was completed between 3 and 9.5 $Å^{-1}$.

2.6. Microbial community analysis

Samples from an oxic sediment, and a Mn reducing sample were taken from both low Np (20 Bq ml^{-1}; 3.2 μM) and high Np (1.3 kBq ml^{-1}; 0.2 mM) microcosms and analysis was performed using PCR based 16S rRNA gene analysis.

2.7. Ribosomal intergenic spacer analysis

DNA was extracted from Np containing microcosm samples (200 μl) using a PowerSoil DNA Isolation Kit (MO BIO Laboratories INC, USA). The 16S 23S rRNA intergenic spacer region from the bacterial RNA operon was amplified as described previously using primers ITSF and ITSReub (Cardinale et al., 2004). The amplified products were separated by electrophoresis in tris acetate EDTA gel. The DNA was stained with ethidium bromide and viewed under short wave UV light. Positive microbial community changes identified by the RISA justified further investigation by DNA sequencing of 16S rRNA gene clone libraries.

2.8. Amplification of 16S rRNA gene sequences

A fragment of the 16S rRNA gene (approximately 1490 b.p.) was amplified from samples using the broad specificity primers 8F (Eden et al., 1991) and 1492R (Lane et al., 1985). PCR reactions were performed in thin walled tubes using a BioRad iCycler (BioRad, UK). Takara Ex Taq Polymerase (Millipore, UK) was used to amplify DNA from the sample extract. The PCR amplification protocol used with the 8F and 1492R primers was: initial denaturation at 94 °C for 4 min, melting at 94 °C for 30 s, annealing at 50 °C for 30 s, elongation at 72 °C for 3 min and 35 cycles, followed by a final extension step at 72 °C for 5 min. The purity of the amplified products was determined by electrophoresis in tris acetate EDTA (TAE) gel. DNA was stained with ethidium bromide and viewed under short wave UV light using a BioRad Geldoc 2000 system (BioRad, UK).

2.9. Cloning

PCR products were purified using a QIAquick PCR purification kit (Qiagen, UK) and ligated directly into a cloning vector containing topoisomerase I charged vector arms (Agilent Technologies, UK) prior to transformation into *Escherichia coli* competent cells expressing Cre recombinase (Agilent Technologies, UK). White transformants that grew on LB agar containing ampicillin and X Gal were screened for an insert using PCR. Primers were complementary to the flanking regions of the PCR insertion site of the cloning vector. The PCR method was: an initial denaturation at 94 °C for 4 min, melting at 94 °C for 30 s, annealing at 55 °C for 30 s, extension at 72 °C for 1 min and 35 cycles, followed by a final extension step at 72 °C for 5 min. The resulting PCR products were purified using an ExoSap protocol, here 2 μl of ExoSap mix (0.058 μl Exonuclease I, 0.5 μl Shrimp Alkaline Phosphatase and 1.442 μl H_2O) was added to 5 μl of PCR product and incubated at 37 °C for 30 min followed by 80 °C for 15 min.

2.10. DNA sequencing and phylogenetic analysis

Nucleotide sequences were determined by the dideoxynucleotide method. An ABI Prism BigDye Terminator Cycle Sequencing Kit was used in combination with an ABI Prism 877 Integrated Thermal Cycler and ABI Prism 377 DNA Sequencer (Perkin Elmer Applied Biosystems, UK). Sequences (typically 900 base pairs in length) were analysed using Mallard (Ashelford et al., 2006) to check for presence of chimeras or sequencing anomalies. Operational taxonomic units (OTU) were determined at a 98% sequence similarity level using Mothur (Schloss et al., 2009). The individual OTU sequences were analysed using the sequencing database of known 16S rRNA gene sequences provided on the Ribosomal Database Project (Cole et al., 2009) to identify nearest neighbours.

3. Results and discussion

3.1. Sediment characteristics

The sediment was dominated by quartz, feldspars (albite and microcline), and sheet silicates (muscovite and chlorite). The sediment had a high Si content (36.3 wt%) and contained Al (6.77%), Fe (3.71%), K (2.67%), Na (0.92%), Mg (0.75%), Ti (0.38%), Ca (0.27%), and Mn (0.09%). The total organic carbon content of the sediment was 0.69% and total carbon was 1.70%. The concentration of 0.5 N HCl extractable Fe in the sediment was 17.1 ± 1.6 mmol kg^{-1} prior to incubation and the sediment pH was ~5.

3.2. Neptunium behaviour during progressive bioreduction

Manganese enriched (2 mM δMnO_2) sediment microcosms amended with electron donor, and a Mn enriched sterile control microcosm, were spiked with 3.2 μM Np(V) and incubated over a 38 day period. Modelling of the initial groundwater chemistry in PHREEQC 2 (Specific Ionic Theory (SIT) database) predicted that the speciation of the Np in solution would be predominantly NpO_2^+ (see Supporting information S1). In the sterile control system, the pH remained stable and bulk biogeochemical changes indicative of terminal electron acceptor progression were not observed (Fig. 1A–F). A release of Mn (~0.2 mM) into the groundwater of the sterile control occurred when the sediments were autoclaved (Fig. 1C) which is similar to past studies with this material (Thorpe et al., 2012). In the microbially active Mn rich microcosms, terminal electron accepting processes progressed in the order NO_3^- > Mn > Fe(III) > SO_4^{2-} reduction as expected (Fig. 1B–E). In all microcosms, the pH remained circumneutral (Fig. 1F), NO_3^- decreased to <0.2 mM within 11 days, and porewater Mn increased to between 0.05 and 0.1 mM after 9 days suggesting concomitant NO_3^- and Mn reduction in these systems (Fig. 1B and C). Microbially mediated Fe(III) reduction was then evident after 17 days as indicated by 0.5 N HCl extractable Fe(II) ingrowth to sediments. Importantly, in this system Mn reduction (indicated by Mn(II) in porewaters) occurred independently of any measurable Fe(III) reduction (indicated by a lack of Fe(II) ingrowth to sediments) across three time points (days 7–11; Fig. 1). The addition of 2 mM δMnO_2 to sediments then allowed an extended Mn reducing 'period', distinguished from the Fe(III) reduction, so that Np behaviour could be tracked throughout the stages of early metal reduction. In the sterile control the added Np(V) was partially sorbed to the sediment, with ~22% removed from solution after 7 days (Fig. 1A). Thereafter, the concentration of Np in solution remained stable. Neptunyl sorption has been observed to a similar extent as in earlier studies using comparable sediment systems (Law et al., 2010) and has been attributed to sorption to negatively charged mineral surfaces (e.g. Fe(III) or Mn bearing minerals:

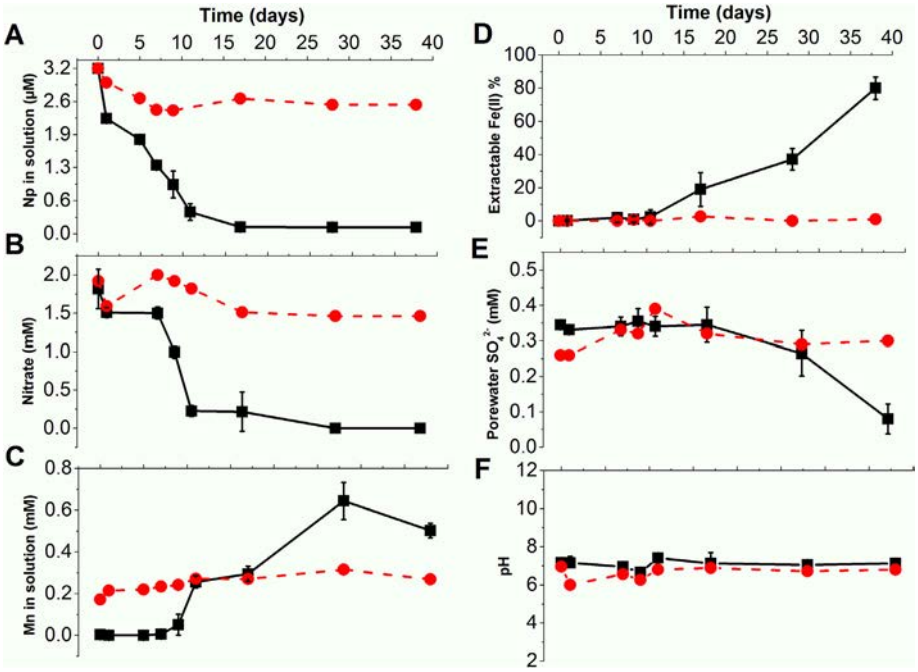

Fig. 1. Microcosm incubation time-series data. (A) Np in porewaters, (B) NO_3 in porewaters, (C) Mn in porewaters, (D) 0.5 N HCl % extractable sedimentary Fe as Fe(II), (E) SO_4^{2} in porewaters, (F) pH. ■ microbially active microcosms; ● sterile control microcosms. Initial pH in all microcosms was ~7. Error bars represent 1σ experimental uncertainty from triplicate microcosm experiments (where not visible error bars are within symbol size).

Combes et al., 1992; Nakata et al., 2002; Arai et al., 2007; Müller et al., 2015; Wilk et al., 2005). In the microbially active microcosms prior to the onset of Mn ingrowth to porewaters (0–7 days), 43.0 ± 1.9% of the added Np was removed from the groundwater (Fig. 1A). By day 11 where Mn reducing conditions had developed, 86.0 ± 4.9% of the added Np had been removed from solution. By the end of the experiment, following Fe(III) and subsequent SO_4^{2-} reduction at 38 days, 96.1 ± 0.5% of the added Np was removed to the sediment. Enhanced removal of Np in active systems, compared to the sterile control, as observed in the first 7 days and prior to the onset of Mn reduction, could be attributed to either reduced surface reactivity in autoclaved sediments and/or enhanced Np sorption in the system with microbial cells present (Gorman Lewis et al., 2005; Ams et al., 2013). Results then show a clear relationship between Np(V) removal from solution and Mn reduction and confirms that Np(V) is significantly removed from groundwater under Mn reducing conditions. It remains unclear in these low concentration Np microcosm studies whether Np(V) removal is linked to microbial metabolism or the result of abiotic reaction with reduced Mn minerals produced by microbes. The formation of Np carbonatohydroxo complexes has been shown to increase the solubility of Np(IV) (Kitamura and Kohara, 2002; Kim et al., 2010). However, in these systems under end point sulphate reducing conditions (pE 4), and taking into account the increase in inorganic carbon expected from acetate utilisation (2 mM), solution modelling in PHREEQC 2 (SIT database) predicted that Np would be speciated as $Np(OH)_4$ (see Supporting information S2).

3.3. *Neptunium L_{III} edge XAS experiments*

To assess the speciation of Np in sediment microcosms under different biogeochemical conditions, select samples were run at the elevated concentrations required for XAS analysis (oxic, nitrate, Mn, Fe(III), sulphate, progressive Mn and sterilised Mn reducing microcosms). The XANES of Np in the sterile, oxic control sediment and in the NO_3^- reducing sediment both showed a Np(V) like spectra displaying the characteristic multiple scattering resonance structure at the high energy flank of the white line resulting from scattering along the axial oxygen atoms of the linear neptunyl moiety (Fig. 2; Moyes et al., 2002; Denecke et al., 2005). Removal of Np from solution in both the oxic and nitrate reducing systems at circumneutral pH is occurring and is likely due to Np(V) sorption to Fe or Mn mineral surfaces (e.g. Combes et al., 1992; Nakata et al., 2002; Wilk et al., 2005; Arai et al., 2007; Law et al.,

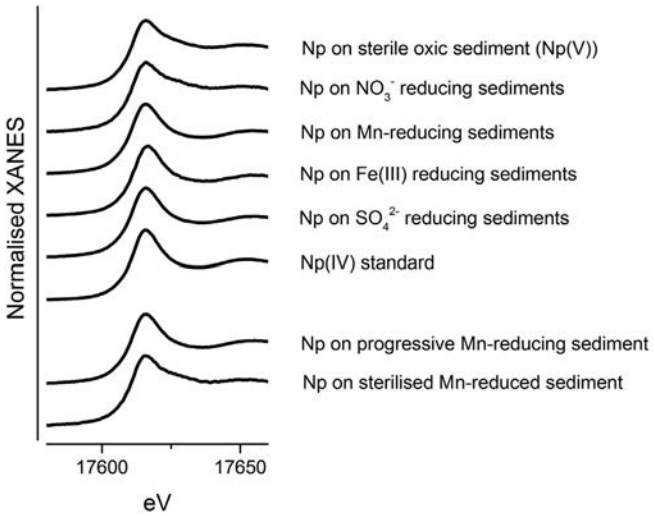

Fig. 2. Np L_{III} edge XANES spectra for Np amended sediments under different biological conditions. Spectra from oxic sediment, nitrate-reducing sediment and sterilised Mn-reducing sediment samples show the Np(V) like multiple scattering resonance structure resulting from high energy scattering along the axial oxygen atoms of the linear neptunyl moiety. Spectra from Mn-, Fe(III)-, sulphate- and progressive Mn-reducing sediment samples do not contain this feature and are therefore more typical of Np(IV) XANES.

2010; Müller et al., 2015). By contrast, the XANES spectra for the progressive Mn reducing microcosm, and the poised Mn , Fe(III) , and SO_4^{2-} reducing systems showed Np(IV) like features with a loss of the multiple scattering resonance structure due to the loss of the two neptunyl dioxygenyl oxygen backscatterers (Fig. 2). Here, the enhanced removal of Np from solution compared to the oxic or nitrate reducing systems is attributed to reductive precipitation of Np(V) to Np(IV) (Law et al., 2010). In the absence of defined (ma trix matched) standards for these complex systems, linear combi nation fitting of the microbially active Mn reducing systems (both progressively reduced, and poised), using the oxic sediment and the sulphate reducing sediment as end members, indicated that Np(IV) was indeed the dominant oxidation state in both systems (>90% Np(IV)) (Ravel and Newville, 2005). In contrast, the XANES spectra for the sterile Mn reduced microcosm was Np(V) like (>90% Np(V)). Interestingly, the presence of significant Np(IV) (~90%) in the microbially active Mn reducing systems and dominant Np(V) (~90%) in the sterile Mn reducing sediments suggests that micro bial reduction of Np(V) to Np(IV) is significant in reductive immo bilisation of Np(V). Any artefacts associated with mineral reactivity and reducing capacity of the sterile Mn reducing sediment result ing from autoclaving cannot however be ruled out here, but the significant change in Np(V) reduction between the microbially active and sterile sediments suggests enzymatic processes are likely to play a role in controlling Np(V) reductive immobilisation. These observations on sterile Mn reducing sediments differ from those observed in a sterilised Fe(III) reducing sediment reacted with Np(V), which facilitated Np(V) reduction (Law et al., 2010).

EXAFS data were also collected from the sterile oxic and microbially active Mn , and SO_4^{2-} reducing samples. The k^3 weighted EXAFS spectra and their Fourier transform spectra are shown together with the corresponding best model fits (Fig. 3; Table 1). The best fit to the sterilised oxic control sample was a Np(V) like coordination environment with two axial oxygen backscatterers at 1.86 Å and four equatorial oxygen backscatterers at 2.45 Å (Table 1, Fig. 3). The distances for both axial and equatorial oxygen backscatterers are within the range reported for Np(V)

Table 1
EXAFS modelling of Np L_{III} edge spectra for Np associated with sediments under different biogeochemical conditions.

	Path	Type	*CN*	*R* (Å)	σ^2 (Å^2)	X_v^2	*R*
Oxic	1	O	2	1.86	0.006	59.8	0.0079
	2	O	4	2.45	0.021		
Mn red	1	O	8	2.31	0.014	217.3	0.0130
Sul red	1	O	8	2.34	0.012	98.9	0.0227

CN is the coordination number, *R* is the interatomic distance, σ^2 is the Debye Waller factor (Å^2), X_v^2 reduced chi square value and *R* is the least squares residual and is a measure of the overall goodness of fit.

(1.82–1.88 Å; Combes et al., 1992; Moyes et al., 2002; Denecke et al., 2005; Arai et al., 2007; Herberling et al., 2008; Law et al., 2010). The statistical relevance of additional shells, containing Fe, Mn, or Np, was assessed using an F test (Ravel and Newville, 2005) and it was found that no significant improvement to the model fit could be achieved. The sulphate reducing sample was modelled using a Np(IV) like coordination environment with eight oxygen back scatterers at a distance of 2.34 Å (Table 1, Fig. 3; Llorens et al., 2005; Law et al., 2010). In agreement with the linear combination fitting, the best fit for the microbially active Mn reducing sample was a Np(IV) like coordination environment, like the sulphate reducing system, with eight oxygen backscatterers at a distance of 2.31 Å. As with the oxic sediment sample, the addition of a second shell of Fe, Np or Mn did not significantly improve the fit when using the F test as a measure of validity. Finally, it is noteworthy that in the samples where significant Np(IV) was present and where EXAFS was possible (the Mn reducing sediment and sulphate reducing microbially active sediments (Fig. 3)), there was no evidence for a Np – O – Np interaction of the type that would be expected for nano particulate NpO_2, which has recently been observed in envi ronmentally relevant systems (Husar et al., 2015). These observa tions are in agreement with past work in sediment systems (Law et al., 2010) which do not show significant evidence for a Np–O–Np interaction.

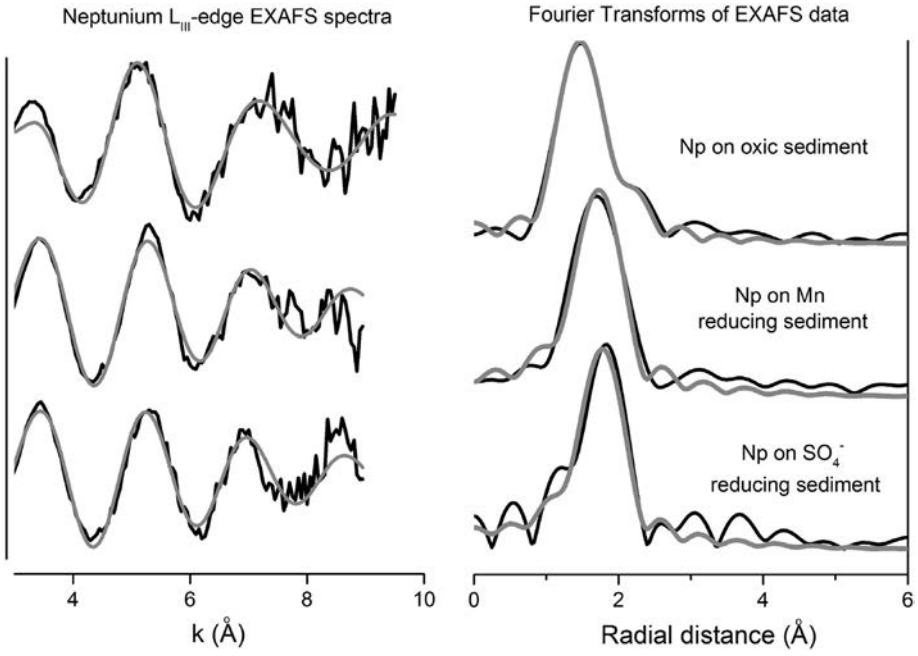

Fig. 3. EXAFS spectra and Fourier transforms (uncorrected for phase shift of backscattering atoms) for Np on sediments under different geochemical conditions. From top to bottom: oxic, Mn- and sulphate-reducing conditions. Black lines are k^3-weighted data and grey lines are the best model fits to the data.

3.4. Microbial community analysis

Analysis of the microbial community in the Mn reducing systems with low (3.2 μM) and high (0.2 mM) Np content was performed to provide insight into the toxicity of Np(V) in these systems. The biogeochemical trajectory was similar in sediments with both low and high concentrations of Np, suggesting that the toxicity of Np in these systems was not significant. These observations were supported by the RISA results, which were similar across both low and high concentration Np amended metal reducing samples, and clone libraries for the same samples, again confirming broadly similar communities (Fig. 4). Both high and low concentration Np experiments did however show a decrease in biodiversity compared to the oxic sediment sample (clone libraries from the oxic sediment showed 34 operational taxonomic units (OTUs) from 71 clones whereas the biostimulated samples showed 7 OTUs from 92 clones in the low Np sample and 12 OTUs from 74 clones in the high Np sample). The clone libraries of both low and high Np concentration Mn reducing samples were dominated (>50%) by members of the class *Bacillus*, including known denitrifying species consistent with the microcosms being primed with 2 mM nitrate prior to Mn reduction.

4. Conclusions

Overall these data show that microbially mediated Mn reduction can lead to reductive immobilisation of Np(V) to Np(IV). The addition of bioavailable δMnO_2 provides a useful approach for prolonging microbial Mn reduction and allowing discrimination between the impacts of microbially mediated Mn and Fe(III) reduction on radionuclide biogeochemistry. Removal of Np during Mn reduction was further maintained during Fe(III) and sulphate reduction and near complete removal of Np from solution had occurred by the onset of sulphate reduction. XANES data confirmed reduction to Np(IV) when Np(V) was exposed to microbially active Mn , Fe(III) , and sulphate reducing sediments. Thermodynamically, Mn reduction is a more favourable process than Fe(III) reduction and so is likely to occur prior to Fe(III) reduction in subsurface environments where electron donor is limited. Although not conclusive these results imply that Np(V) reduction in these systems occurs in the presence of a viable microbial population rather than abiotically, through reaction with reduced Mn bearing minerals. Reduction of Np(V) by metal reducing bacteria may provide an additional mechanism for Np(V) removal from groundwater ahead of the development of robust Fe(III) reducing conditions. Results show the importance of subsurface microbial manganese cycling on the speciation of neptunium. These data have relevance to the fundamental understanding of Np behaviour in the shallow and deep subsurface.

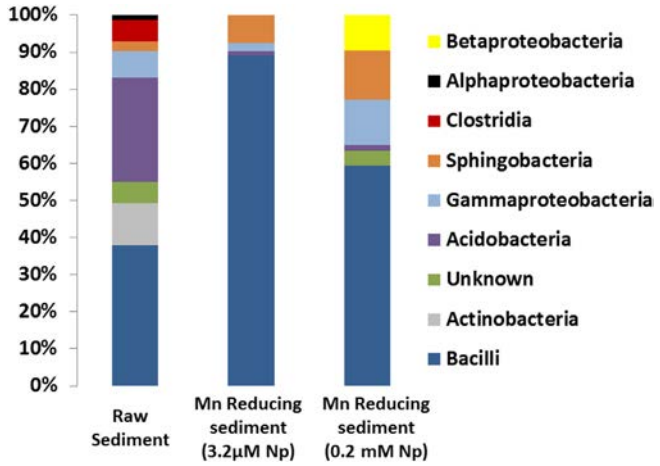

Fig. 4. Microbial community analysis of: oxic 'raw' sediment at 0 days; Mn-reducing sediment amended with 3.2 μM ^{237}Np; Mn-reducing sediment amended with 0.2 mM ^{237}Np.

Acknowledgements

This work has been supported by the Natural Environmental Research Council grants 'BIGRAD' – Biogeochemical Gradients and Radionuclide Transport (NE/H0077668/1) and 'LO RISE' – Long lived Radionuclides in the Surface Environment (NE/L000547/1; part of the RATE programme (Radioactivity and the Environment) co funded by the Environment Agency and Radioactive Waste Management Ltd.), an EPSRC University of Manchester/Sellafield Ltd. KTA award for which we acknowledge Nick Atherton and the Sellafield Land Quality Team, and STFC award ST/K001787/1. We thank Paul Lythgoe and Alastair Bewsher at The University of Manchester, and Jorg Rothe (KIT INE) for help with data acquisition. Beamtime was obtained from the ANKA Lightsource (proposal number ANS 85) with support from the EU Actinet Programme.

References

Ams, D.A., Swanson, J.S., Szymanowski, J.E.S., Fein, J.B., Richmann, M., Reed, D.T., 2013. The effect of high ionic strength on neptunium(V) adsorption to a halophilic bacterium. Geochim. Cosmochim. Acta 110, 45 57.

Arai, Y., Moran, P.B., Honeyman, B.D., Davis, J.A., 2007. In situ spectroscopic evidence for neptunium(V)-carbonate inner-sphere and outer-sphere ternary surface complexes on hematite surfaces. Environ. Sci. Technol. 41, 3940 3944.

Ashelford, K.E., Chuzhanova, N.A., Fry, J.C., Jones, A.J., Weightman, A.J., 2006. New screening software shows that most recent large 16S rRNA gene clone libraries contain chimeras. Appl. Environ. Microbiol. 72, 5734 5741.

Bach, D., Christiansen, B.C., Schild, D., Geckeis, H., 2014. TEM study of green rust sodium sulfate (GRNa.SO_4) interacted with neptunyl ions (NpO_2^+). Radiochim. Acta 102 (4), 279 290.

Behrends, T., Krawczyk-Barsch, E., Arnold, T., 2012. Implementation of microbial processes in the performance assessment of spent nuclear fuel repositories. Appl. Geochem. 27, 453 462.

Cantrell, K.J., 2009. Transuranic Contamination in Sediment and Groundwater at the U.S. DOE Hanford Site. US Department of Energy Report: PNNL-18640. Available at: http://www.pnl.gov/main/publications/external/technical_reports/PNNL-18640.pdf.

Cardinale, M., Brusetti, L., Quatrini, P., Borin, S., Puglia, A.M., Rizzi, A., Zanardini, E., Sorlini, C., Corselli, C., Daffonchio, D., 2004. Comparison of different primer sets for use in automated ribosomal intergenic spacer analysis of complex bacterial communities. Appl. Environ. Microbiol. 70, 6147 6156.

Choppin, G.R., Stout, B.E., 1989. Actinide behaviour in natural waters. Sci. Total Environ. 83, 203 216.

Choppin, G.R., 2007. Actinide speciation in the environment. J. Radioanal. Nucl. Chem. 273, 695 703.

Cole, J.R., Wang, Q., Cardenas, E., Fish, J., Chai, B., Farris, R.J., Kulam-Syed-Mohideen, A.S., McGarrell, D.M., Marsh, T., Garrity, G.M., Tiedje, J.M., 2009. The ribosomal database project: improved alignments and new tools for rRNA analysis. Nucleic Acids Res. 37, 141 145.

Combes, J.M., Chisholm-Brause, C.J., Brown, G.E., Parks, G.A., Conradson, S.D., Eller, P.G., Triay, I.R., Hobart, D.E., Miejer, A., 1992. EXAFS spectroscopic study of neptunium(V) sorption at the α-iron hydroxide oxide α-FeOOH/water interface. Environ. Sci. Technol. 26 (2), 376 382.

Denecke, M.A., Dardenne, K., Marquardt, C.M., 2005. Np(IV)/Np(V) valence determinations from Np L3-edge XANES/EXAFS. Talanta 65, 1008 1014.

Eden, P.E., Schmidt, T.M., Blakemore, R.P., Pace, N.R., 1991. Phylogenetic analysis of *Aquaspirillum magnetotacticum* using polymerase chain reaction-amplified 16S rRNA-specific DNA. Int. J. Syst. Bacteriol. 41, 324 325.

Fredrickson, J.K., Balkwill, D.L., 2006. Geomicrobial processes and biodiversity in the deep terrestrial subsurface. Geomicrobiol. J. 23, 345 356.

Gadd, G.M., 2010. Metals, minerals and microbes: geomicrobiology and bioremediation. SGM prize lecture. Microbiol. 156, 609 643.

Gorman-Lewis, D., Fein, J.B., Soderholm, L., Jensen, M.P., Chiang, M.H., 2005.

Experimental study of neptunyl adsorption onto Bacillus subtilis. Geochim. Cosmochim. Acta 69, 4837 4844.
Goto, K., Taguchi, S., Fukue, Y., Ohta, K., Watanabe, H., 1997. Spectrophotometric determination of manganese with 1-(2-pyridylazo)-2-naphthol and a non-ionic surfactant. Talanta 24, 752 753.
Herberling, F., Denecke, M.A., Bosbach, D., 2008. Neptunium(V) co-precipitation with calcite. Environ. Sci. Technol. 42 (2), 471 476.
Hu, Y., Schwaiger, L.K., Booth, C.H., Kukkadapu, R.K., Cristiano, E., Kaplan, D., Nitsche, H., 2010. Molecular interactions of plutonium(VI) with synthetic manganese-substituted goethite. Radiochim. Acta 98, 655 663.
Husar, R., Hübner, R., Hennig, C., Martin, P.M., Chollet, M., Weiss, S., Stumpf, T., Zanker, H., Ikeda-Ohno, A., 2015. Intrinsic formation of nanocrystalline neptunium dioxide under neutral aqueous conditions relevant to deep geological repositories. Chem. Commun. 51, 1301 1304.
Icopini, G.A., Boukhalfa, H., Neu, M.P., 2007. Biological reduction of Np(V) and Np(V) citrate by metal-reducing bacteria. Environ. Sci. Technol. 41 (8), 2764 2769.
Kaszuba, J.P., Runde, W.H., 1999. The aqueous geochemistry of neptunium: dynamic control of soluble concentrations with applications to nuclear waste disposal. Environ. Sci. Technol. 33, 4427 4433.
Kim, B.Y., Oh, J.Y., Baik, M.H., Yun, J.I., 2010. Effect of carbonate on the solubility of neptunium in natural granitic groundwater. Nuc. Eng. Technol. 42 (5), 552 561.
Kitamura, A., Kohara, Y., 2002. Solubility of neptunium(IV) in carbonate media. J. Nucl. Sci. Technol. 3, 294 297.
Lane, D.J., Pace, B., Olsen, G.J., Stahl, D.A., Sogin, M.L., Pace, N.R., 1985. Rapid determination of 16S ribosomal-RNA sequences for phylogenetic analysis. Proc. Natl. Acad. Sci. 82, 6955 6959.
Law, G.T.W., Geissler, A., Lloyd, J.R., Livens, F.R., Boothman, C., Begg, J.D.C., Denecke, M.A., Rothe, J., Dardenne, K., Burke, I.T., Charnock, J.M., Morris, K., 2010. Geomicrobiological redox cycling of the transuranic element neptunium. Environ. Sci. Technol. 44, 8924 8929.
Llorens, I., Den Auwer, C., Moisy, P., Ansoborlo, E., Vidaud, C., Funke, H., 2005. Neptunium uptake by serum transferrin. FEBS J. 272, 1739 1744.
Lloyd, J.R., Yong, P., Macaskie, L.E., 2000. Biological reduction and removal of Np(V) by two microorganisms. Environ. Sci. Technol. 34, 1297 1301.
Lloyd, J.R., Chesnes, J., Glasauer, S., Bunker, D.J., Livens, F.R., Lovley, D.R., 2002. Reduction of actinides and fission products by Fe(III)-reducing bacteria. Geomicrobiol. J. 19, 103 120.
Lloyd, J.R., 2003. Microbial reduction of metals and radionuclides. FEMS Microbiol. Rev. 27, 411 425.
Lloyd, J.R., Renshaw, J.C., 2005. Bioremediation of radioactive waste: radionuclide-microbe interactions in laboratory and field-scale studies. Curr. Opin. Biotechnol. 16, 254 260.
Lovley, D.R., Phillips, E.J.P., 1988. Manganese inhibition of microbial iron reduction in anaerobic sediments. Geomicrobiol. J. 6, 145 155.
Lovley, D.R., Phillips, E.J.P., 1987. Rapid assay for microbially reducible ferric iron in aquatic sediments. Appl. Environ. Microbiol. 53, 1536 1540.
Morris, K., Butterworth, J.C., Livens, F.R., 2000. Evidence for the remobilization of sellafield waste radionuclides in an intertidal salt marsh, West Cumbria, UK. Estuar. Coast. Shelf Sci. 51, 613 625.
Moyes, L.N., Jones, M.J., Reed, W.A., Livens, F.R., Charnock, J.M., Mosselmans, J.F.W., Hennig, C., Vaughan, D.J., Pattrick, R.A.D., 2002. An X-ray absorption spectroscopy study of neptunium(V) reactions with mackinawite (FeS). Environ. Sci. Technol. 36, 179 183.
Müller, K., Groschel, A., Rossberg, A., Bok, F., Franzen, C., Brendler, V., Foerstendorf, H., 2015. In situ spectroscopic identification of neptunium(V) inner-sphere complexes on the hematite water interface. Environ. Sci. Technol. 49, 2560 2567.
Nakata, K., Nagasaki, S., Tanaka, S., Sakamoto, Y., Tanaka, T., Ogawa, H., 2002. Sorption and reduction of neptunium(V) on the surface of iron oxides. Radiochim. Acta 90 (9 11), 665 669.
Newsome, L., Morris, K., Lloyd, J.R., 2014. The biogeochemistry and bioremediation of uranium and other priority radionuclides. Chem. Geo. 363, 164 184.
Pedersen, K., 2000. Exploration of deep intraterrestrial microbial life: current perspectives. FEMS Microbiol. Lett. 185, 9 16.
Powell, B.A., Duff, M.C., Kaplan, D.I., Field, R.A., Newville, M., Hunter, D.B., Bertsh, P.M., Coates, J.T., Eng, P., Rivers, M.L., Serkiz, S.M., Sutton, S.R., Triay, I.R., Vaniman, D.T., 2006. Plutonium oxidation and subsequent reduction by Mn(IV) minerals in Yucca Mountain tuff. Environ. Sci. Technol. 140 (11), 3508 3514.
Ravel, B., Newville, M., 2005. ATHENA, ARTEMIS, HEPHAESTUS: data analysis for X-ray absorption spectroscopy using IFEFFIT. J. Synchrotron. Radiat. 12, 537 541.
Renshaw, J.C., Butchins, L.J.C., Livens, F.R., May, I., Charnock, J.M., Lloyd, J.R., 2005. Bioreduction of uranium: environmental implications of a pentavalent intermediate. Environ. Sci. Technol. 39, 5657 5660.
Rizoulis, A., Steele, H.M., Morris, K., Lloyd, J.R., 2012. The potential impact of microbial metabolism during the geodisposal of intermediate level waste. Min. Mag. 76, 3261 3270.
Ruggiero, C.E., Boukhalfa, H., Forsythe, J.H., Lack, J.G., Hersman, L.E., Neu, M.P., 2005. Actinide and metal toxicity to prospective bioremediation bacteria. Environ. Microbiol. 7, 88 97.
Stamper, A., McKinlay, C., Coughlin, D., Laws, F., 2013. Groundwater Annual Report 2012. Sellafield Ltd, Technical Report: LQTD000032.
Schloss, P.D., Westcott, S.L., Ryabin, T., Hall, J.R., Hartmann, M., Hollister, E.B., Lesniewski, R.A., Oakley, B.B., Parks, D.H., Robinson, C.J., Sahl, J.W., Stres, B., Thallinger, G.G., Van Horn, D.J., Weber, C.F., 2009. Introducing mothur: open-source, platform-independent, community-supported software for describing and comparing microbial communities. Appl. Environ. Microbiol. 75, 7537 7541.
Songkasiri, W., Reed, D.T., Rittmann, B.E., 2002. Bio-sorption of neptunium(V) by Pseudomonas fluorescens. Radiochim. Acta 90, 785 789.
Thorpe, C.L., Law, G.T.W., Boothman, C., Lloyd, J.R., Burke, I.T., Morris, K., 2012. Synergistic effect of high nitrate concentrations on sediment bioreduction. Geomicrobiol. J. 29, 484 493.
Viollier, E., Inglett, P.W., Hunter, K., Roychoudhury, A.N., Van Cappellen, P., 2000. The ferrozine method revisited: Fe(II)/Fe(III) determination in natural waters. Appl. Geochem. 15, 785 790.
Wang, Z., Lee, S.W., Kapoor, P., Tebo, B.M., Giammar, D.E., 2013. Uraninite oxidation and dissolution induced by manganese oxide: a redox reaction between two insoluble minerals. Geochim. Cosmochim. Acta 100 (1), 24 40.
Wang, Z., Xiong, W., Tebo, B.M., Giammar, D.E., 2014. Oxidative UO_2 dissolution induced by soluble Mn(III). Environ. Sci. Technol. 48 (1), 289 298.
Wilk, P.A., Shaughnessy, D.A., Wilson, R.E., Nitsche, H., 2005. Interfacial interactions between Np(V) and manganese oxide minerals manganite and hausmannite. Environ. Sci. Technol. 39, 2608 2615.
Wilkins, M.J., Livens, F.R., Vaughan, D.J., Beadle, I., Lloyd, J.R., 2007. The influence of microbial redox cycling on radionuclide mobility in the subsurface at a low-level radioactive waste storage site. Geobiol. 5, 293 301.
Williamson, A.J., Morris, K., Shaw, S., Byrne, J.M., Boothman, C., Lloyd, J.R., 2013. Microbial reduction of Fe(III) under alkaline conditions relevant to geological disposal. Appl. Environ. Microbiol. 79 (11), 3320 3326.